# Second approximation coefficient for the binary distribution function of ions for the primitive model of an electrolyte solution

Nagat Abdel-Rahman Hussein
*Mathematics Department, Faculty of Science, Assiut University, Assiut, Egypt*

Abdel-Nasser Abdel-Maugood Osman
*Mathematics Department, Faculty of Science at Qena, Qena, Egypt*
(Received 29 June 1993; revised manuscript received 19 December 1994)

The purpose of this paper is to solve analytically and numerically the second approximation coefficient in the density expansion of the binary distribution function. A generalized analytic formula can be obtained for the second approximation coefficient. The analytic formula is computed numerically for the restricted primitive model of an electrolyte solution. Then the numerical solution of the second approximation coefficient is compared with its approximate analytic results. Moreover the numerical solution is compared with the available Monte Carlo data, hypernetted chain approximations, and with other results for three primitive-model (1-1, 2-1, and 2-2) electrolyte solutions.

PACS number(s): 82.60.Lf, 05.20.−y, 61.20.−p

## I. INTRODUCTION

The binary distribution function (BDF) is one of the most important functions of statistical mechanics. The earliest integral equation theories for the BDF for hard spheres were due to Born, Green, and Yevick [1]. The Kirkwood superposition approximation, when applied to the stationary Bogoliubov-Born-Green-Kirkwood-Yvon (BBGKY) hierarchy [2], gives rise to the Born-Green-Yvon (BGY) equation. In a recent article [3] the BGY integral equation for hard spheres had been studied by using two closures that provide improvements to the traditional Kirkwood superposition. For the time being, the primitive model (PM) is the most well studied model of electrolyte solutions. The hypernetted chain (HNC) approximation has been published [4] and the BDF investigated in real electrolyte solutions by the application of the PM.

In several review articles [5–8], Wheaton has solved the fundamental statistical mechanical (BBGKY) hierarchy. Representing the electrolyte solution with the chemical model along with his technique, Wheaton obtained expressions for the BDF for both dilute and concentrated solutions. By using the PM to represent the electrolyte solution we could obtain, analytically, an expression for the solution of the second approximation coefficient (SAC) by using the three-dimensional Fourier integral [9] for its solution. Computationally convenient theoretical approximations for the SAC are used. Our purpose is to carry out an analysis that gives the analytical and the numerical solution for calculation of the SAC.

The outline of this paper is as follows. In Sec. II we derive an analytical expression for the SAC. Our analytic results are compared to the available Monte Carlo (MC) [10,11] data and with many theoretical results for the PM of 1-1 electrolyte solutions. In Sec. III we solve the SAC numerically. In this section we are specifically concerned with the accuracy of the numerical solution of the SAC in calculating the density expansion of the BDF. We then compare in detail the numerical solution with a more refined treatment embodied in the HNC approximation [11] and MC calculations. Our calculations are restricted to the cases where some results of MC and HNC calculations are available for comparison.

## II. ANALYTICAL SOLUTION

### A. Density expansion for the binary distribution function

According to the PM, let each ion in the solution be represented by a charged hard sphere with a center-to-center distance $a_{ij}$. The direct potential between ions $i$ and $j$ with ionic charges $e_i$ and $e_j$, respectively, and separated by a distance $r$ is given by

$$\psi_{ij}=V_{ij}+V_{ij}^{*}\ , \tag{2.1}$$

where $V_{ij}=z_i z_j e^2/Dr$ is the Coulomb potential with the dielectric constant $D$. $z_i$ and $z_j$ are the valences of ions of type $i$ and $j$ and $e$ is the magnitude of electronic charge. The short-range potential $V_{ij}^{*}$ is defined by

$$V_{ij}^{*}=\begin{cases}\infty\ , & r\le a_{ij}\ \ [\text{thus } \exp(-\beta V_{ij}^{*})=0]\ ,\\ 0\ , & r>a_{ij}\ \ [\text{thus } \exp(-\beta V_{ij}^{*})=1]\ ,\end{cases} \tag{2.2}$$

where $\beta=1/kT$, $K_B$ is Boltzmann's constant, and $T$ is the absolute temperature. The basic idea of constructing a convergent expansion for the BDF goes back to the work of Schmitz [12,13]. Bogoliubov's density expansion for the BDF is [2,14,15]

 

$$F_{ij}(r)=\exp(-\beta V_{ij}-\beta V_{ij}^{*}) \times\left[1+\sum_k n_k\int_0^{\infty} dr_k\{[\exp(-\beta V_{ik}-\beta V_{ik}^{*})-1][\exp(-\beta V_{jk}-\beta V_{jk}^{*})-1]\}+O(n^2)\right],$$

$$n_k=\nu_k n=\nu_k N/V\ , \quad (2.3)$$

where $n_i$ is the density of ions of type $i$, $\nu$ ($\equiv\nu_+ +\nu_-$) is the number of cations (positive ions) $\nu_+$ and anions (negative ions) $\nu_-$ produced by dissociation of one molecule of the electrolyte, and $N$ is the total number of ions in the volume $V$. Using the density expansion due to Bogoliubov [14] and Schmitz's iteration procedure [13], Ebeling and Krienke [16] obtained a general expression for the density expansion of the BDF, which, in the region $r>a$, has the form [17]

$$F_{ij}(r)=\exp[G_{ij}(r)]\left[1+\sum_k n_k\int dr'(\{\exp[G_{ik}(r')]-1\}\{\exp[G_{jk}(|r-r'|)]-1\} -G_{ik}(r)G_{jk}(|r-r'|))+O(n^2)\right],\quad r>a\ . \quad (2.4)$$

The function $G_{ij}(r)$ is the pair correlation function with a distance $r$ between a particle of species $i$ and a particle of species $j$. The pair correlation function may be written, in terms of Debye-Hückel $\kappa$, the parameters $x=\kappa r$ and $t=\kappa a$, and the plasma parameter $\varepsilon$ ($\equiv e^2\kappa/Dk_BT$), as

$$G_{ij}(x)=\varepsilon q_{ij}(e^{-x}/x)\ , \quad q_{ij}=q_{ji}=-z_iz_j\left[\frac{e^t}{1+t}\right]\ . \quad (2.5)$$

The Debye-Hückel $\kappa$ is defined by [4]

$$\kappa=\left[\frac{4\pi}{Dk_BT}\sum_i n_ie_i^2\right]^{1/2}\ . \quad (2.6)$$

Similarly, one can write the density expansion of the BDF [Eq. (2.4)] in terms of the parameter $x=\kappa r$ as

$$F_{ij}(x)=\exp[G_{ij}][1+\Omega_{ij}(x)+O(n^2)]\ . \quad (2.7)$$

The contribution of the second-order term can be written as

$$\Omega_{ij}(x)=\frac{1}{\kappa^3}\sum_k n_k\int[C_{ik}(x')C_{jk}(|x-x'|) -G_{ik}(x')G_{jk}(|x-x'|)]dx'\ , \quad (2.8)$$

where

$$C_{ik}(x')=\exp[G_{ik}(x')]-1\ . \quad (2.9)$$

The function $C_{jk}(x')$ can be obtained from Eq. (2.9) by changing the indices $i$ and $k$ to $j$ and $k$ and the variable $x'$ to $|x-x'|$. The expression (2.8) will be denoted by the second approximation coefficient. In the next following subsection, the three-dimensional Fourier transformations will be used to obtain an explicit expression for its analytic solution.

### B. Second approximation coefficient

In this section we shall point out the method for evaluating an explicit expression for the analytical solution of the SAC [Eq. (2.8)]. By substituting the three-dimensional Fourier transformation, which is [9]

$$C_{ik}(x')=\left[\frac{1}{2\pi}\right]^3\int C_{ik}(p)e^{i\mathbf{p}\cdot\mathbf{x}'}dp\ , \quad p=|\mathbf{p}|\ , \quad (2.10)$$

into Eq. (2.8) and taking into account the inverse Fourier transformations

$$C_{ik}(p)=\int e^{-i\mathbf{p}\cdot\mathbf{x}'}C_{ik}(x')dx'^3\ , \quad (2.11)$$

we get

$$\Omega_{ij}(p)=\frac{1}{\kappa^3}\sum_k n_k[C_{ik}(p)C_{jk}(p)-G_{ik}(p)G_{jk}(p)]\ . \quad (2.12)$$

Since we are only interested in the range of values $t\le x<\infty$, the solution of Eq. (2.12) will require a knowledge of $\Omega_{ij}(x)$ within this range. Using Taylor series expansion, we can rewrite the right-hand side of Eq. (2.9) as

$$C_{ik}(x')=\sum_{\alpha=1}^{\infty}\frac{(\varepsilon q_{ik})^{\alpha}}{\alpha!}\frac{e^{-\alpha x'}}{x'^{\alpha}}\ . \quad (2.13)$$

Substituting this result into the integral equation defined by Eq. (2.11), we get

$$C_{ik}(p)=4\pi\sum_{\alpha=1}\frac{(\varepsilon q_{ik})^{\alpha}}{\alpha!}\Phi_{ik}(p,\alpha)\ , \quad (2.14)$$

where

$$\Phi_{ik}(p,\alpha)=\int_{t_{ik}}^{\infty}e^{-\alpha x'}x'^{-(\alpha-1)}\frac{\sin(px')}{p}dx'\ , \quad t_{ik}=\kappa a_{ik}\ . \quad (2.15)$$

Now it is convenient to introduce a new variable, say, $u$ such that $x'=u+t_{ik}$; substituting this into Eq. (2.15) we obtain

$$\Phi_{ik}(p,\alpha)=e^{-\alpha t_{ik}}t_{ik}^{-(\alpha-1)}\sum_r(-1)^r\frac{(\alpha-1)_r}{r!}t_{ik}^{-r}\Pi_{ik}(p,\alpha)\ , \quad (2.16)$$

where $(\alpha-1)_r=(\alpha-2+r)!/(\alpha-2)!$; (see Ref. [9]). According to Eqs. (2.15) and (2.16) it is obvious that the function $\Pi_{ik}(p,\alpha)$ has the form

$$\Pi_{ik}(p,\alpha)=\left[\frac{1}{p}\right]\left[\sin(pt_{ik})\int_0^\infty u^r e^{-\alpha u}\cos(pu)du + \cos(pt_{ik})\int_0^\infty u^r e^{-\alpha u}\sin(pu)du\right] . \tag{2.17}$$

The function $\Pi_{ik}(p,\alpha)$ is the sum of two integrals; one of them is simply the Laplace transform [9] of $\sin(pu)$ and the other is the Laplace transform of $\cos(pu)$ with respect to the variable $u$. The problem thus reduces to the evaluation of the two integrals, on the right-hand side of Eq. (2.17), which are easily solved to give

$$\Pi_{ik}(p,\alpha)=(-1)^r\frac{\partial^r}{\partial\alpha^r}\Gamma_{ik}(p,\alpha) , \tag{2.18}$$

where

$$\Gamma_{ik}(p,\alpha)=\frac{1}{p}\left[\frac{\alpha\sin(pt_{ik})}{p^2+\alpha^2}+\frac{p\cos(pt_{ik})}{p^2+\alpha^2}\right] . \tag{2.19}$$

Consequently, one can obtain an expression for the function $C_{ik}(p)$ by the combination of Eqs. (2.14), (2.16), and (2.18); thus we have

$$C_{ik}(p)=4\pi\sum_{\alpha=1}\frac{\eta_{ik}^{\alpha}}{\alpha!}\sum_{r=0}\frac{(\alpha-1)_r}{r!}\bar{t}_{ik}^{(r-1)}\frac{\partial^r}{\partial\alpha^r}F_{ik}(p,\alpha) ,$$

$$\eta_{ik}=\frac{\varepsilon q_{ik}}{t_{ik}e^{t_{ik}}} , \quad \alpha=1,2,3,4,\ldots . \tag{2.20}$$

The calculation of $C_{jk}(p)$ is quite analogous to that for $C_{ik}(p)$. From Eqs. (2.5) and (2.13), it is seen that $G_{ik}(p)$ can be obtained directly by substituting $\alpha=1$ into Eq. (2.20). Rewriting the function $\Omega_{ij}(p)$ by substituting $C_{ik}$, $C_{jk}$, $G_{ik}$, and $G_{jk}$ into Eq. (2.12), we find

$$\Omega_{ij}(p)=\frac{16\pi^2}{\kappa^3}\sum_k n_k\left[\sum_{\gamma=1}\sum_{s=0}\sum_{\alpha=1}\sum_{r=0}\frac{(\alpha-1)_r}{r!}\frac{(\gamma-1)_s}{s!}\frac{\eta_{ik}^{\alpha}}{\alpha!}\frac{\eta_{jk}^{\gamma}}{\gamma!}t_{ik}^{-(r-1)}\bar{t}_{jk}^{(s-1)}\times\left[\frac{\partial^r}{\partial\alpha^r}\frac{\partial^s}{\partial\gamma^s}\Pi(p,\alpha,\gamma)\right]-\eta_{ik}\eta_{jk}\Pi(p,\alpha=\gamma=1)\right] \tag{2.21}$$

[see Eq. (2.16)] , where

$$\Pi(p,\alpha,\gamma)=\Gamma_{ik}(p,\alpha)\Gamma_{jk}(p,\gamma) . \tag{2.22}$$

The function $\Gamma_{jk}(p,\gamma)$ can be obtained from $\Gamma_{ik}(p,\alpha)$ by changing the indices $i$ and $k$ to $j$ and $k$ and the variable $\alpha$ to $\gamma$. It is easy to verify that the function $\Pi(p,\alpha,\gamma)$ can be written in an explicit form by substituting the functions $\Gamma_{ik}(p,\alpha)$ and $\Gamma_{jk}(p,\gamma)$ into Eq. (2.22), such that

$$\Pi(p,\alpha,\gamma)=F_1(p,\alpha,\gamma)+F_2(p,\alpha,\gamma)+F_3(p,\alpha,\gamma) , \tag{2.23}$$

where

$$F_1(p,\alpha,\gamma)=\alpha\gamma\left[\frac{\cos(pt_3)-\cos(pt_4)}{p^2(p^2+\alpha^2)(p^2+\gamma^2)}\right] , \quad t_3=t_{ik}-t_{jk} , \quad t_4=t_{ik}+t_{jk} \tag{2.24}$$

$$F_2(p,\alpha,\gamma)=\frac{1}{2p(p^2+\alpha^2)(p^2+\gamma^2)}\{\alpha[\sin(pt_3)+\sin(pt_4)]-\gamma[\sin(pt_3)-\sin(pt_4)]\} , \tag{2.25}$$

and

$$F_3(p,\alpha,\gamma)=\left[\frac{\cos(pt_3)+\cos(pt_4)}{2(p^2+\alpha^2)(p^2+\gamma^2)}\right] . \tag{2.26}$$

The function $\Omega_{ij}(p)$ can then be solved by taking the inverse Fourier transformation of $\Omega_{ij}(p)$ to find $\Omega_{ij}(x)$. Our aim now is to simplify the inverse Fourier transformations, for Eq. (2.21), by dividing it into simplified terms. Now applying the inverse Fourier transformation Eq. (2.11), one can write Eq. (2.24) as

$$F_1(x,\alpha,\gamma)=\frac{\alpha\gamma}{4\pi^2}\int_0^\infty p\left[\frac{\cos(pt_3)-\cos(pt_4)}{p^2(p^2+\gamma^2)(p^2+\gamma^2)}\right]\frac{\sin(px)}{x}dp . \tag{2.27}$$

If we use the partial fractions for the quantity in square brackets on the right-hand side of this equation, we obtain

$$F_1(x,\alpha\neq\gamma)=\frac{1}{8\pi}\frac{1}{\gamma^2-\alpha^2}\{-\gamma(e^{-\alpha x}/\alpha x)[\cosh(\alpha t_3)-\cosh(\alpha t_4)]+\alpha(e^{-\gamma x}/\gamma x)[\cosh(\gamma t_3)-\cosh(\gamma t_4)]\} , \tag{2.28}$$

where the integrations are performed with respect to the variable $p$. We can also evaluate the functions $F_2(x,\alpha,\gamma)$ and $F_3(x,\alpha,\gamma)$ via a method closely analogous to that used in evaluating the function $F_1(x,\alpha\neq\gamma)$. The results are outlined

here as

$$F_2(x,\alpha\neq\gamma)=\frac{1}{8\pi}\frac{\alpha-\gamma}{\gamma^2-\alpha^2}\{(e^{-\alpha x}/\alpha x)[\sinh(\alpha t_3)]-(e^{-\gamma x}/\gamma x)[\sinh(\gamma t_3)]\}$$
$$+\frac{1}{8\pi}\frac{\alpha+\gamma}{\gamma^2-\alpha^2}\{(e^{-\alpha x}/\alpha x)[\sinh(\alpha t_4)-(e^{-\gamma x}/\gamma x)[\sinh(\gamma t_4)]\} \tag{2.29}$$

and

$$F_3(x,\alpha\neq\gamma)=\frac{1}{8\pi}\frac{1}{\gamma^2-\alpha^2}\{(e^{-\alpha x}/x)[\cosh(\alpha t_3)+\cosh(\alpha t_4)]-(e^{-\gamma x}/x)[\cosh(\gamma t_3)+\cosh(\gamma t_4)]\} . \tag{2.30}$$

In light of the above-mentioned results Eqs. (2.28)–(2.30), one can construct a formula for the function $\Pi(x,\alpha,\gamma)$ by substituting the indicated equations into the inverse Fourier transformation of Eq. (2.23) to obtain

$$\Pi(x,\alpha\neq\gamma)=\frac{1}{8\pi}\left[\frac{2}{\gamma^2-\alpha^2}\right]\{\gamma[(e^{-\alpha x}/\alpha x)\sinh(\alpha t_{jk})][\sinh(\alpha t_{ik})+\cosh(\alpha t_{ik})]$$
$$-\alpha[(e^{-\gamma x}/\gamma x)\sinh(\gamma t_{ik})][\sinh(\gamma t_{jk})+\cosh(\gamma t_{jk})]$$
$$+[(e^{-\alpha x}/x)\cosh(\alpha t_{jk})][\sinh(\alpha t_{ik})+\cosh(\alpha t_{ik})]$$
$$-[(e^{-\gamma x}/x)\cosh(\gamma t_{ik})][\sinh(\gamma t_{jk})+\cosh(\gamma t_{jk})]\} , \quad \alpha\neq\gamma . \tag{2.31}$$

It should be noted that this equation is satisfied for all values of $\alpha$ and $\gamma$ except for those ($\alpha=\gamma$) that make $\Pi(x,\alpha,\gamma)$ divergent. This divergence is due to the factor $[1/(\gamma^2-\alpha^2)]$, which has a singularity at equal values of $\alpha$ and $\gamma$. We can derive an expression for the function $\Pi(x,\alpha=\gamma)$ in terms of the functions $\Gamma_{ik}(p,\alpha)$ and $\Gamma_{jk}(p,\gamma)$, assuming that $\alpha=\gamma$. Then Eqs. (2.24)–(2.26) may be written in the forms

$$F_1(p,\alpha=\gamma)=\frac{\alpha^2}{2p^2(p^2+\alpha^2)^2}[\cos(pt_3)-\cos(pt_4)] , \tag{2.32}$$

$$F_2(p,\alpha=\gamma)=\frac{\alpha\sin(pt_4)}{p(p^2+\alpha^2)^2} , \tag{2.33}$$

and

$$F_3(p,\alpha=\gamma)=\frac{1}{2(p^2+\alpha^2)^2}[\cos(pt_3)+\cos(pt_4)] . \tag{2.34}$$

In a manner identical to that used above we can obtain a general formula for the function $\Pi(x,\alpha=\gamma)$. It can be proved that

$$\Pi(x,\alpha=\gamma)=\frac{1}{8\pi\alpha}\{(e^{-\alpha x}/\alpha x)[e^{\alpha(t_{ik}+t_{jk})}-\cosh(t_{ik}-t_{jk})\alpha]$$
$$-(e^{-\alpha x}/x)[(t_{ik}+t_{jk})e^{\alpha(t_{ik}+t_{jk})}]+(e^{-\alpha x})(e^{\alpha(t_{ik}+t_{jk})})\} . \tag{2.35}$$

It should be noted that the results represented by Eqs. (2.31) and (2.35) are very important in determining the SAC in the density expansion of the BDF. It is obvious that the function $\Pi(x,\alpha\neq\gamma)$ has to be treated differently from $\Pi(x,\alpha=\gamma)$. This is displayed clearly in Eqs. (2.31) and (2.35).

The procedure of separating the function $\Omega_{ij}(x)$ into two parts is used to obtain elegant formal results or series expansions that are ordered in terms of ordering parameters. In terms of the results (2.31) and (2.35) we can rewrite the inverse Fourier transformation of $\Omega_{ij}(P)$ as

$$\Omega_{i,j}(x)=\frac{2\pi}{\kappa^3}\sum_k n_k\left[2\sum_{\alpha=1}\sum_{s=0}\sum_{\gamma=1}\sum_{r=0}\frac{(\alpha-1)_r}{r!}\frac{(\gamma-1)_s}{s!}\frac{1}{\alpha!\gamma!}\left[\frac{\varepsilon q_{ik}}{t_{ik}e^{t_{ik}}}\right]^\alpha\left[\frac{\varepsilon q_{jk}}{t_{jk}e^{t_{jk}}}\right]^\gamma t_{ik}^{-(r-1)}t_{jk}^{-(s-1)}\frac{\partial^r}{\partial\alpha^r}\frac{\partial^s}{\partial\gamma^s}\right.$$
$$\times(\{(e^{-\alpha(x-t_{ik})}/x)[\cosh(\alpha t_{jk})+(\gamma/\alpha)\sinh(\alpha t_{jk})]$$
$$-(e^{-\gamma(x-t_{jk})}/x)[\cosh(\gamma t_{ik})+(\alpha/\gamma)\sinh(\gamma t_{ik})]\}/(\gamma^2-\alpha^2))$$
$$+\sum_{\alpha=2}\sum_{u=0}\left[\frac{(\alpha-1)_u}{\alpha!u!}\right]^2\left[\frac{\varepsilon q_{ik}}{t_{ik}e^{t_{ik}}}\right]^\alpha\left[\frac{\varepsilon q_{jk}}{t_{jk}e^{t_{jk}}}\right]^\alpha(t_{ik}t_{jk})^{-(u-1)}\frac{\partial^{2u}}{\partial\alpha^{2u}}$$
$$\times(\{(e^{-\alpha x}/\alpha x)[e^{\alpha(t_{ik}+t_{jk})}-\cosh(t_{ik}-t_{jk})\alpha]$$
$$\left.-(e^{-\alpha x}/x)(e^{\alpha(t_{ik}+t_{jk})})(t_{ik}+t_{jk}-x)\}/\alpha)\right] . \tag{2.36}$$

The summations introduced in this expansion include all the different combinations of $\alpha$ and $\gamma$. Here $\alpha$ and $\gamma$ are both integers. This generalization introduced in Eq. (2.36) will have a considerable use in the following subsection. In the Appendix, a deeper analysis is used to enable us to simplify considerably this expansion.

### C. Density expansion techniques

It is shown in the Appendix that the function $\Omega_{ij}(x)$ can be expanded into powers of $\eta$,

$$\begin{aligned}\Omega_{ij}(x)=\frac{4\pi}{\kappa^3}n_0(\eta t)^2x\{&[\eta\mathcal{H}_1^{(0,1)}(z_1,z_2)\Psi_{0,1}+\eta^2\mathcal{H}_1^{(0,2)}(z_1,z_2)\Psi_{0,2}+\eta^3\mathcal{H}_1^{(0,3)}(z_1,z_2)\Psi_{0,3}\\&+\eta^4\mathcal{H}_1^{(0,4)}(z_1,z_2)\Psi_{0,4}+\eta^5\mathcal{H}_1^{(0,5)}(z_1,z_2)\Psi_{0,5}+\eta^6\mathcal{H}_1^{(0,6)}(z_1,z_2)\Psi_{0,6}]\\&+[\eta\mathcal{H}_1^{(1,0)}(z_1,z_2)\Psi_{1,0}+\eta^3\mathcal{H}_1^{(1,2)}(z_1,z_2)\Psi_{1,2}+\eta^4\mathcal{H}_1^{(1,3)}(z_1,z_2)\Psi_{1,3}\\&+\eta^5\mathcal{H}_1^{(1,4)}(z_1,z_2)\Psi_{1,4}+\eta^6\mathcal{H}_1^{(1,5)}(z_1,z_2)\Psi_{1,5}\\&+\eta^7\mathcal{H}_1^{(1,6)}(z_1,z_2)\Psi_{1,6}+\eta^8\mathcal{H}_1^{(1,7)}(z_1,z_2)\Psi_{1,7}]\\&+[\eta^2\mathcal{H}_1^{(2,0)}(z_1,z_2)\Psi_{2,0}+\eta^3\mathcal{H}_1^{(2,1)}(z_1,z_2)\Psi_{2,1}+\eta^5\mathcal{H}_1^{(2,3)}(z_1,z_2)\Psi_{2,3}\\&+\eta^6\mathcal{H}_1^{(2,4)}(z_1,z_2)\Psi_{2,4}+\eta^7\mathcal{H}_1^{(2,5)}(z_1,z_2)\Psi_{2,5}+\eta^8\mathcal{H}_1^{(2,6)}(z_1,z_2)\Psi_{2,6}]\\&+[\eta^3\mathcal{H}_1^{(3,0)}(z_1,z_2)\Psi_{3,0}+\eta^4\mathcal{H}_1^{(3,1)}(z_1,z_2)\Psi_{3,1}+\eta^5\mathcal{H}_1^{(3,2)}(z_1,z_2)\Psi_{3,2}\\&+\eta^7\mathcal{H}_1^{(3,4)}(z_1,z_2)\Psi_{3,4}+\eta^8\mathcal{H}_1^{(3,5)}(z_1,z_2)\Psi_{3,5}\\&+\eta^9\mathcal{H}_1^{(3,6)}(z_1,z_2)\Psi_{3,6}+\eta^{10}\mathcal{H}_1^{(3,7)}(z_1,z_2)\Psi_{3,7}]\}\\&+\frac{2\pi}{\kappa^3}n_0(\eta t)^2x[\eta^2\mathcal{H}_2^{(1)}(z_1,z_2)\varphi_1+\eta^4\mathcal{H}_2^{(2)}(z_1,z_2)\varphi_2+\eta^6\mathcal{H}_2^{(3)}(z_1,z_2)\varphi_3\\&+\eta^8\mathcal{H}_2^{(4)}(z_1,z_2)\varphi_4+\eta^{10}\mathcal{H}_2^{(5)}(z_1,z_2)\varphi_5+\eta^{12}\mathcal{H}_2^{(6)}(z_1,z_2)\varphi_6]\ ,\end{aligned}\tag{2.37}$$

where the definitions of the coefficients $\mathcal{H}$, $\Psi_{n,m}(y,z)$, and $\varphi_n(y)$ can be found in Eqs. (A7), (A8), (A10), and (A13). Comparisons of the evaluations based on this expression will be made with the numerical solution of $\Omega_{ij}(x)$.

In what follows we have made use of the modified form (DHX) of Debye-Hückel theory in which the distribution function is represented by

$$F_{ij}(x)=\exp(-z_iz_j\varepsilon\{e^{t-x}/[x(1+t)]\})\ .\tag{2.38}$$

Moreover, we have made some of Wheaton's distribution function [8] (derived from the BBGKY hierarchy of equations)

$$F_{ij}(x)=\exp\{z_iz_j\varepsilon[-(\{e^t+(1+t+t^2/2)[\cosh(t)-1]\}/(1+t))e^{-x}/x+0.5[\cosh(t)-1]e^{-x}]\}\ .\tag{2.39}$$

All the computations were carried out with the previous parameters used in the MC calculation by Card and Valleau [10], Valleau and Cohen [18], Valleau, Cohen, and Card [11], and Sloth and Sorensen [4]. The MC calculations have been made for 1-1 electrolytes with $T=298$ K, $a=4.25$ Å, and $D=78.5$ for 2-1 and 2-2 electrolytes with $T=298.16$ K, $a=4.2$ Å, and $D=78.358$. In the following we shall discuss the character of the effects that can be attributed to the inclusion of the higher-order terms in the expansion (2.37) for 1-1, 2-1, and 2-2 electrolytes.

In the first case of 1-1 electrolytes we observed that the valence factors $\mathcal{H}_1^{(n,m)}(z_1,z_2)$ and $\mathcal{H}_2^{(n)}(z_1,z_2)$ have three constant values. These values are either 2, 0, or $-2$ for like and unlike ions according to the exponential values $n$ and $m$ in the expansion (A9). Certain cancellations that take place are due to the charge neutrality, which is based on the fact that like and unlike ions are equal in magnitude but opposite in sign. An interesting feature is that each higher-order coefficient $\Psi_{n,m}$ in the expansion (2.37) is observed to be successively smaller than its predecessor with increasing concentration. Consequently, the combination of Eqs. (2.7) and (2.37) gives reasonably good values for the BDF compared with the so-called DHX results. In this paper we shall restrict our comparisons to the 1-1 case where the series expansion Eq. (2.37) converges quite rapidly for all concentrations of interest in the range of $r$ shown in Figs. 1 and 2. In these figures we examine briefly the BDF and compare its behavior, from the analytical and numerical solutions, with MC results [10] and the CM approximation Eq. (2.39). It is clear from the figures that the analytical and numerical solutions exhibit significantly some deviation in the analytic solution, which is inevitable due to the cutoff approximations in the series expansion (A9).

Unfortunately, in the 2-1 and 2-2 cases, comparisons could not be made. This is interpreted as being due to slow convergence of the expansion (2.37) in the higher valence electrolytes. Consequently, the numerical results for $\Omega_{ij}(x)$ are inadequate for obtaining an accurate distri-

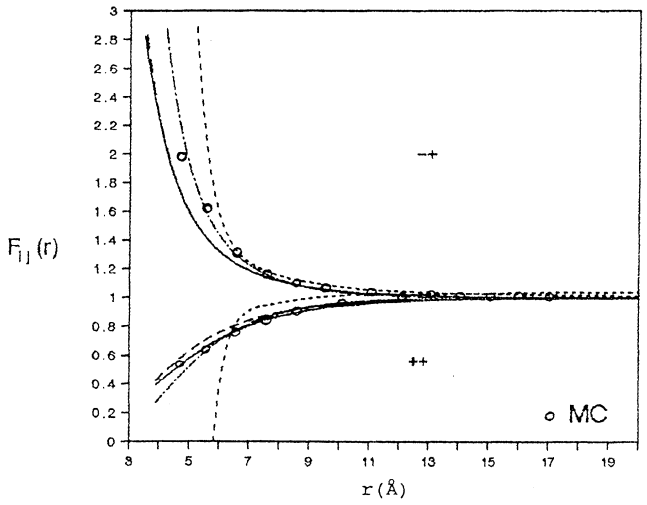


FIG. 1. Binary distribution functions $F_{ij}(r)$ for the 1-1 primitive model at $c=1.0001M$. Full lines and dotted lines represent the numerical and the approximate analytic solutions of Eq. (2.7), respectively. Dashed lines and dot-dashed lines indicate DHX results and Eq. (2.39), respectively.

bution function for higher valence electrolytes. On the other hand, the results for 2-2 electrolytes are a little more precise than the 2-1 results. As a result of this discussion, large departures from HNC approximations and MC points are to be expected for cases of electrolytes of higher valences (2-1 and 2-2).

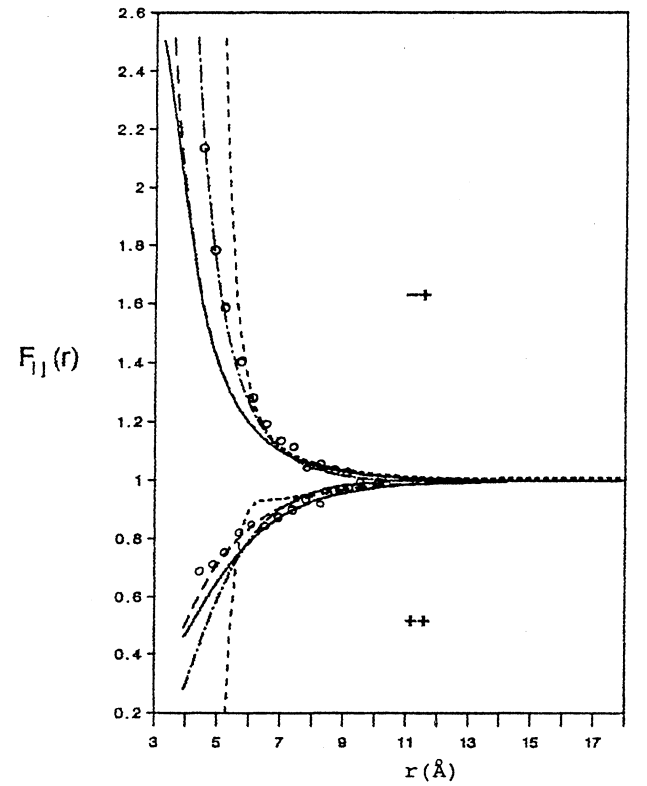


FIG. 2. Binary distribution functions $F_{ij}(r)$ for the 1-1 primitive model at $c=1.9676M$. The symbols have the same meaning as in Fig. 1. The circles indicate the MC results.

The justification of slow convergence for the series expansion given by Eq. (2.37) is based on the following observations: (i) the magnitudes of the valence factors, given by Eqs. (A7) and (A8), respectively, and (ii) the molar concentration values. It is readily seen by direct verification that the valence factors $\mathcal{H}_1^{(n,m)}(z_1,z_2)$ and $\mathcal{H}_2^{(n)}(z_1,z_2)$ are rapidly increasing functions for 2-1 and 2-2 electrolytes. It is important to observe that the magnitudes of these factors increase, for like and unlike ions, with increasing exponentials $n$ and $m$ in the expansion (A9). Moreover, the coefficients $\Psi_{n,m}$ and the subsequent terms have more and more power of small parameters that increase for concentration values lower than $0.0625M$. In our opinion, these are the reasons why the series expansion (2.37) does not converge quickly enough for higher valence electrolytes.

In general, we observe that the analytical solution results given here have the disadvantage that they converge much more slowly for the 2-1 and 2-2 electrolytes than in the case of 1-1 electrolytes. However, this disadvantage is offset by a numerical solution method requiring much fewer calculations per iterations. In Sec. III we shall sketch the derivation of the basic formula for the numerical calculation of $\Omega_{ij}(x)$ within the framework of the BDF approximations.

## III. NUMERICAL SOLUTION

### A. Numerical treatment

The application of the PM to the density expansion of the BDF has made possible the calculation of the SAC numerically. It is shown in Eq. (2.7) that the function $F_{ij}(x)$ vanishes in the range $x<\kappa a$. The numerical solution of $\Omega_{ij}(x)$ for the PM follows as an immediate consequence, and since $\Omega_{ij}(x)$ decreases rapidly with increasing $x$, it is expected that the numerical results should be convenient for the numerical solution to the BDF. By introducing bipolar coordinates in Eq. (2.8), the SAC for the PM may be rewritten as

$$\Omega_{ij}(x)=\frac{2\pi}{\kappa^3 x}\sum_k n_k[\omega_1(x,t)-\omega_2(x,t)]\ , \tag{3.1}$$

where

$$\omega_1(x,t)=\int_{\kappa a}^{\infty} uC_{ik}(u)du\int_{|u-x|}^{u+x} sC_{jk}(s)ds \tag{3.2}$$

and

$$\omega_2(x,t)=\int_{\kappa a}^{\infty} uG_{ik}(u)du\int_{|u-x|}^{u+x} sG_{jk}(s)ds\ . \tag{3.3}$$

This is because the BDF vanishes exactly for $x$ less than some finite range $x=\kappa r<\kappa a$. In order to study the properties of the integral (3.2), it is convenient to substitute the functions $C_{ik}(x')$ and $C_{jk}(|x-x'|)$ into this integral (3.2). Substituting the results of $\omega_1(x,t)$ and $\omega_2(x,t)$ into Eq. (3.1) yields an expression for the function $\Omega_{ij}(x)$ that depends explicitly on the pair potential functions. The final result is

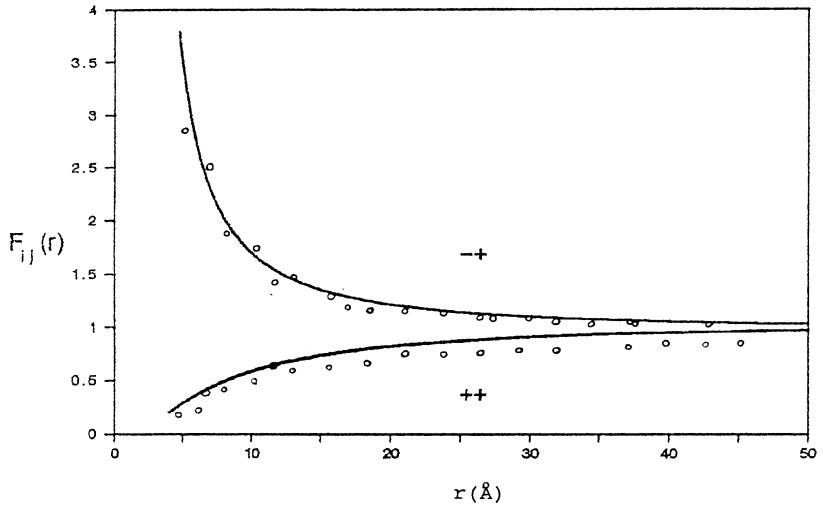


FIG. 3. $F_{++}$ and $F_{-+}$ functions for 1-1 electrolytes with $c=0.00911M$. The circles indicate the Monte Carlo points. Full lines indicate DHX results, Eq. (2.39), and the numerical solution of Eq. (2.7). The results are in excellent agreement for the concentration value studied.

$$\Omega_{ij}(x)=\frac{2\pi}{\kappa^3 x}\sum_k n_k\left\{\int_0^{e^{-\kappa a}}dy\frac{\ln y}{y}\left[\exp\left[\varepsilon_{ik}\frac{y}{\ln y}\right]-1\right]\int_{-\ln y+x}^{|-\ln y-x|}ds\left[\exp\left[-\varepsilon_{jk}\frac{e^{-s}}{s}\right]-1\right]\right.$$
$$\left.-z_i z_j z_k^2(\varepsilon q)^2[-e^{-2t}+1+2(x-t)](e^{-x}/2)\right\},\quad \varepsilon_{ik}=-\varepsilon q_{ik}\ . \tag{3.4}$$

This integral has the property of relating $C_{ik}(x')$ and $C_{jk}(|x-x'|)$ functions over the range $(0,e^{-\kappa a})$. This would be an interesting formula for which detailed results were found numerically by applying the trapezoidal integration rule. This method is a possible alternative and has the advantage that less computer memory is needed and that it is easier to incorporate different $F_{ij}(x)$ with different valences. It is also noted that for the parameters used in the present calculations, no divergence problems were found by the method outlined here.

### B. Results

The BDF for a number of PM 1-1 and 2-2 electrolytes was published quite some years ago [11] and here we discuss primarily some of the most interesting features found for 1-1, 2-1, and 2-2 electrolytes in the PM with equal ion sizes. For this reason, results for these valence types electrolytes are of great importance. This is due to the fact that the stronger interactions offer a more stringent test of our numerical solution of $\Omega_{ij}(x)$. The function $\Omega_{ij}(x)$ defined by the result (3.4) was solved numerically and after substituting into the density expansion Eq. (2.7), the numerical results were compared with the HNC approximations [11] and MC calculations. In Figs. 3 and 6 the functions $F_{-+}$ and $F_{++}$ for 1-1 and 2-1 electrolytes with $C=0.009\,11M$ are shown. First, it is noted that the results obtained by Eqs. (2.38) and (2.39) are in excellent agreement with the numerical solution of Eq. (2.7) for the concentration value studied. For comparison we also show the MC results for the most dense systems. In Figs. 1–5 the numerical solution of the BDF

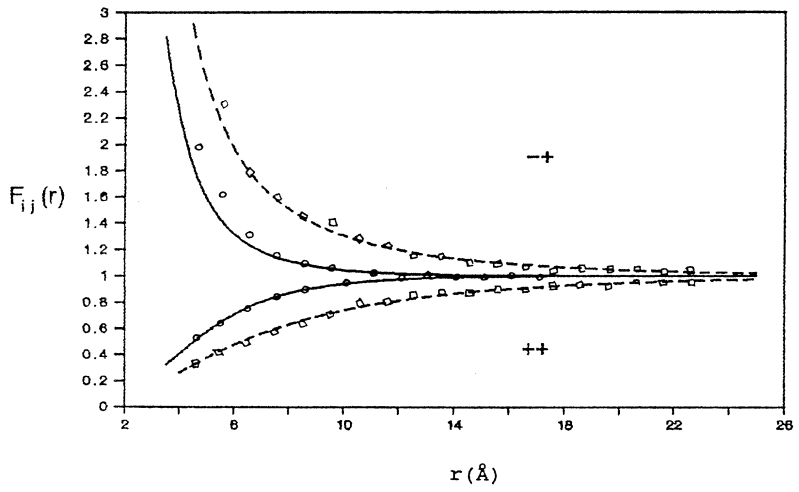


FIG. 4. $F_{++}$ and $F_{-+}$ functions for 1-1 electrolytes. Dashed lines and full lines indicate the numerical solution of Eq. (2.7) for $c=0.103\,76M$ and $1.0001M$, respectively. Circles and squares indicate the Monte Carlo points.

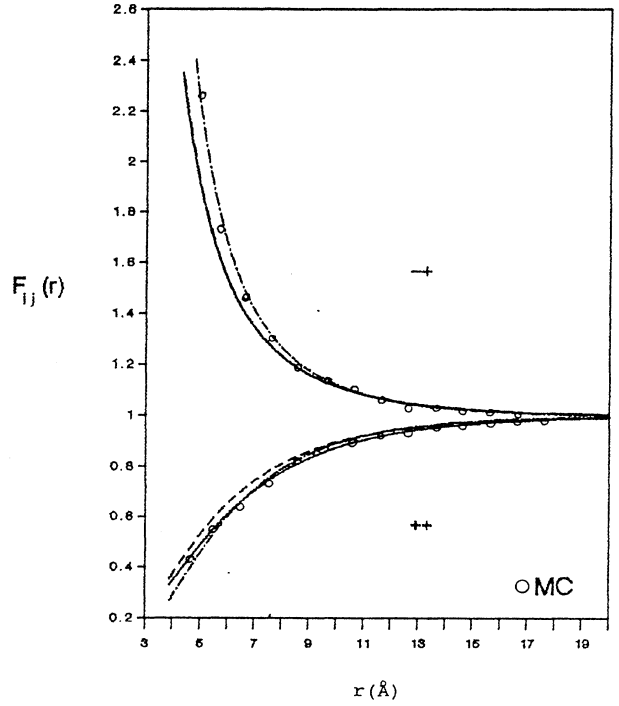


FIG. 5. Like and unlike binary distribution functions $F_{++}$ and $F_{-+}$ for the 1-1 primitive model at 0.425 02$M$. DHX results, Eq. (2.39), and the numerical solution of Eq. (2.7) are indicated by dashed lines, dot-dashed lines, and full lines, respectively.

is shown for a 1-1 electrolyte with $C=0.009\,11M$, $0.103\,76M$, $0.425\,02M$, $1.0001M$, and $1.9676M$. It is also obvious that the numerical solution curves represented by $F_{++}$ values agree more closely with the MC points than the $F_{-+}$ values at all the above-mentioned concentrations, but this agreement is worse for the concentration $1.9676M$. On the other hand, it is apparent from Figs. 3 and 4 that the numerical solution of the BDF is in closest agreement with the MC points.

Our numerical solution for the BDF, in the case of 2-1 electrolytes ($C=0.009\,11M$ and $1.9676M$), is shown in Figs. 6 and 7, respectively. However, at high concentration ($C=1.9676M$), Fig. 7 shows the variation in the numerical solution results that is observed when compared with the DHX results and Wheaton's approximations for the BDF.

The 2-2 results are most interesting and are displayed in Figs. 8 and 9. Similar comparisons were made for the 2-2 electrolyte with concentrations ($C=0.0625M$ and $2.0M$). This can readily be seen from Figs. 8 and 9, where the corresponding grand canonical MC results of Valleau, Cohen and Card [11] are also indicated for comparison. Clearly the BDF results show poor agreement with the MC points. However, the CM results and DHX curves are somewhat better than the numerical solution curves compared with the MC points. For further comparison we also examine the HNC results for the BDF function with our numerical solution of Eq. (2.7). It is clear from the results in Figs. 8 and 9 that some deviations are found between the numerical solution and the HNC results. Focusing on the like and unlike charge correlations, i.e., on $F_{-+}$ and $F_{++}$ in the present case of interest, one may expect that the SAC results are not completely sufficient, as is clear from the figures. This may be due to some aspects of the solution structure of models for 2-2 electrolytes in the higher concentration range. On the other hand, in the case of like ions, concerning $F_{++}$, we observed that our numerical results are superior to those of Wheaton's results, for 1-1 electrolytes, while this does not hold for the 2-2 electrolytes. These deviations could be due to differences between the PM and CM approximations. This might explain the difference between the numerical solution curves, MC points, and Wheaton's curves.

In conjunction with the previous results of the BDF, it is seen that the CM results for 1-1 electrolytes in the case of different ions (i.e., $F_{-+}$) are in surprisingly good agreement with the MC points. Thus it seems as if the CM in fact offers a better description of $F_{-+}$ than the PM represented by Eq. (2.7) and DHX results. More-

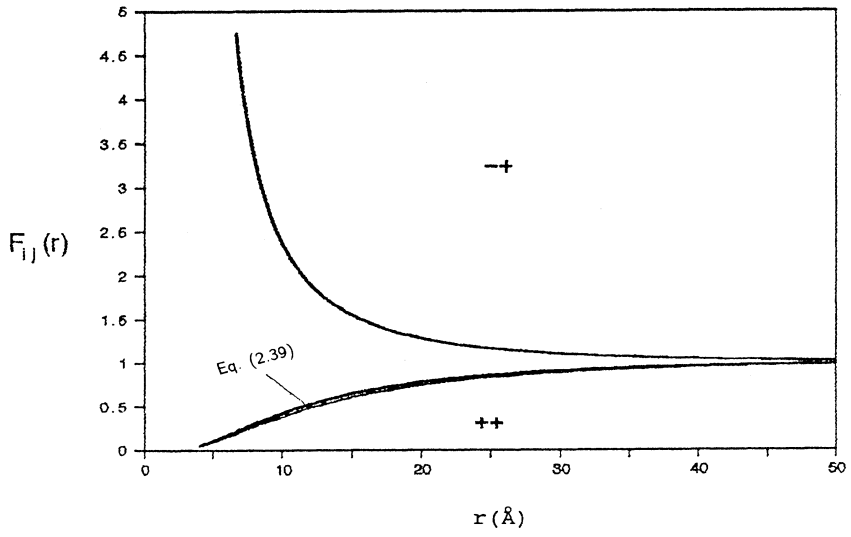


FIG. 6. Like and unlike binary distribution functions $F_{++}$ and $F_{-+}$ for the 2-1 primitive model at 0.009 11$M$. Full lines indicate DHX results, Eq. (2.39), and the numerical solution of Eq. (2.7). The results show the same qualitative behavior as in Fig. 3.

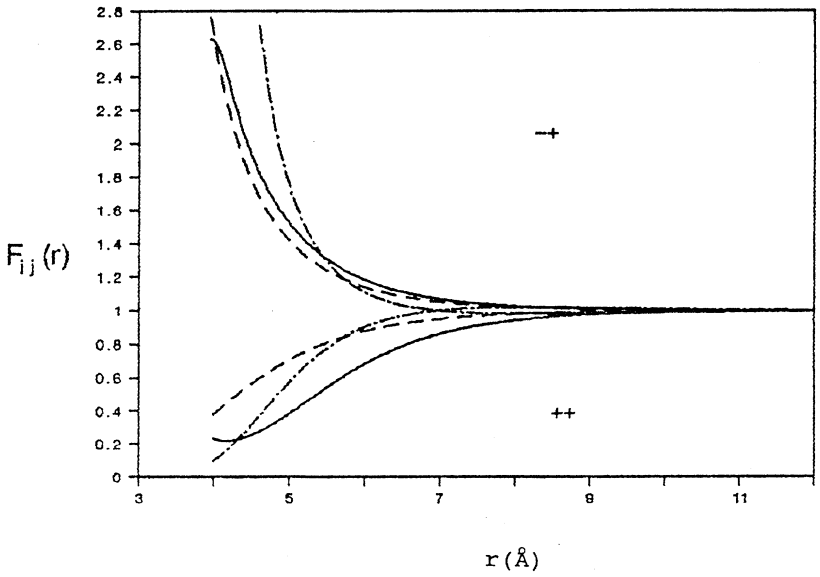


FIG. 7. Like and unlike binary distribution functions $F_{++}$ and $F_{-+}$ for the 2-1 primitive model at $1.9676M$. DHX results, Eq. (2.39), and the numerical solution of Eq. (2.7) are indicated by dashed lines, dot-dashed lines, and full lines, respectively.

over, Figs. 1–6 and 8 show that the PM and CM approximations give closely corresponding results as measured by $F_{++}$ over a wide range of concentrations. It has already been shown that all of the $F_{++}$ functions, investigated in Figs. 1–9, are increasing functions with distance at least in the intervals shown here. This implies that the repulsive electrostatic forces dominate whenever two anions are close to each other.

## IV. CONCLUSION

In light of the results outlined above and the interest in evaluating the numerical results of $\Omega_{ij}(x)$ in this paper, we present a brief conclusion for the main results obtained by solving $\Omega_{ij}(x)$ by two different methods. The first method is the analytical method, discussed in Sec. II. This method leads to some difficulties. Attention must be paid to the effect of truncation error in the evaluation of the numerical results for each term in the expansion (2.37). The convergence of these terms, for 2-1 and 2-2 electrolytes, to the final numerical result of the expansion (2.37) is slow. We also evaluated $\Omega_{ij}(x)$ via a numerical solution method that was discussed in Sec. III. The numerical solution outlined here greatly facilitates the solution of $\Omega_{ij}(x)$ for the PM of 1-1, 1-2, and 2-2 electrolyte solutions for concentrations between $0.009\,11M$ and $2.0M$. The numerical solution presented in this paper

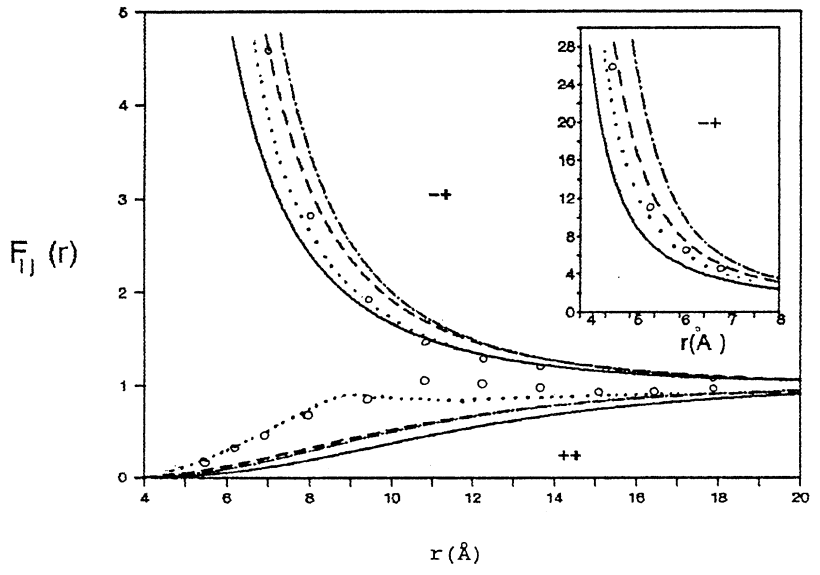


FIG. 8. Binary distribution functions $F_{++}$ and $F_{-+}$ for the 2-2 primitive model at $0.0625M$. The MC results are indicated by circles. DHX results, Eq. (2.39), and the numerical solution of Eq. (2.7) are indicated by dashed lines, dot-dashed lines, and full lines, respectively. Dotted lines indicate the HNC results.

has no difficulties and the numerical results are found to be in excellent agreement with the MC points for 1-1 electrolytes for some concentration values. Moreover, the numerical solution of $\Omega_{ij}(x)$ is known exactly over the entire range shown in Eq. (3.4). This equation enables the accuracy of the numerical technique to be evaluated over the entire range. From the comparison between the analytical and numerical solution of the BDF given by Eq. (2.7), it is clear that the numerical solution of Eq. (2.7) is very accurate compared with its approximate analytical solution.

## APPENDIX: SIMPLIFIED PROPERTIES FOR THE DISTRIBUTION FUNCTION

The function $\Omega_{ij}(x)$ will then be transformed to a form more useful by making use of the assumptions

$$\alpha x = y \ , \quad \gamma x = z \ . \tag{A1}$$

Moreover, the following relations in the special case of symmetric electrolytes are assumed to be valid:

$$n_1 = n_2 = n_0 \ , \quad a_{11} = a_{12} = a_{22} = a \ , \quad t_{11} = t_{12} = t_{22} = t \ . \tag{A2}$$

It is clear from the result (2.36) that the function $\Omega_{ij}(x)$ connects a particle of species $i$ at location 1 and a particle of species $j$ at location 2 with a particle of species $k$ at location 3. Proceeding with a summation over the index $k$ and taking into consideration the previous conceptions (A1) and (A2), Eq. (2.36) can be reformulated as

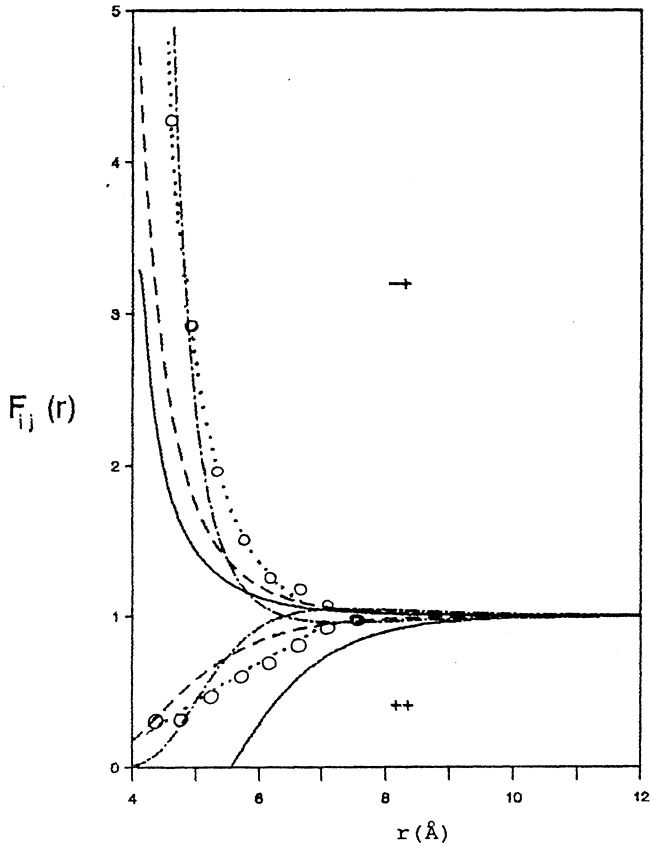


FIG. 9. Binary distribution functions $F_{++}$ and $F_{-+}$ for the 2-2 primitive model at $c = 2.0M$. Symbols have the same meaning as in Fig. 8.

$$\Omega_{ij}(x) = \frac{2\pi}{\kappa^3} n_0 x \left[ 2 \sum_{m=0} \sum_{s=0} \sum_{n=0} \sum_{r=0} \frac{(n)_r}{r!} \frac{(m)_s}{s!} \eta^{n+m+2} \frac{\mathcal{H}_1^{(n,m)}(z_1,z_2)}{(n+1)!(m+1)!} t^2 \left[ \frac{1}{\xi} \right]^{r+s} \frac{\partial^r}{\partial y^r} \frac{\partial^s}{\partial z^s} \mathcal{F}(y,z) \right.$$
$$\left. + \sum_{n=1} \sum_{u=0} \left[ \frac{(n)_u}{u!} \right]^2 \left[ \frac{t}{(n+1)!} \right]^2 \left[ \frac{1}{\xi} \right]^{2u} \eta^{2n} \mathcal{H}_2^{(n)}(z_1,z_2) \frac{\partial^{2u}}{\partial y^{2u}} \mathcal{B}(y) \right] \ , \quad \alpha = n+1 \ , \quad \gamma = m+1 \ , \tag{A3}$$

where

$$\eta = \frac{\varepsilon q}{t e^t} \ , \quad \xi = t/x \ , \quad \alpha t = \xi y \ , \quad \gamma t = \xi z \ , \tag{A4}$$

$$\mathcal{F}(y,z) = \left[ e^{-y(1-\xi)} \left[ \cosh(\xi y) + \frac{z}{y} \sinh(\xi y) \right] - e^{-z(1-\xi)} \left[ \cosh(\xi z) + \frac{y}{z} \sinh(\xi z) \right] \right] \Big/ (z^2 - y^2) \ , \tag{A5}$$

and

$$\mathcal{B}(y) = [(e^{-y}/y)(e^{2\xi y} - 1) + (e^{-y(1-2\xi)})(1-2\xi)]/y \ . \tag{A6}$$

The valence factors are defined by

$$\mathcal{H}_1^{(\alpha,\gamma)}(z_1,z_2) = \nu_1(-z_1^2)^\alpha (-z_1 z_2)^\gamma + \nu_2(-z_2^2)^\gamma (-z_1 z_2)^\alpha \tag{A7}$$

and

$$\mathcal{H}_2^{(\alpha)}(z_1,z_2) = (-z_1 z_2)^\alpha [\nu_1(-z_1^2)^\alpha + \nu_2(-z_2^2)^\alpha] \ . \tag{A8}$$

Our method of calculating the numerical values of $\Omega_{ij}(x)$ is based on the expansion as a convergent power series in the $\eta$ parameter. For different $n$ and $m$ values the function $\Omega_{ij}(x)$ will be written in terms of a set of functions denoted by $\Psi_{n,m}$ and $\varphi_n$ as

$$\Omega_{ij}(x)=\frac{2\pi}{\kappa^3}n_0(\eta t)^2 x\left[2\sum_{n=0}\sum_{m=0}\mathcal{H}_1^{(n,m)}(z_1,z_2)\Psi_{n,m}(y,z)\eta^{n+m}+\sum_{n=1}\mathcal{H}_2^{(n)}(z_1,z_2)\varphi_n(y)\eta^{2n}\right],\quad n=\alpha-1\ ,\quad m=\gamma-1\ , \tag{A9}$$

where

$$\Psi_{n,m}(y,z)=\frac{1}{(m+1)!}\sum_{s=0}\frac{(m)_s}{s!}\left[\frac{1}{\xi}\right]^s\psi_n^{(s)}(y,z)\ . \tag{A10}$$

The function $\psi_n^{(s)}(y,z)$ takes the form

$$\psi_n^{(s)}(y,z)=\frac{1}{(n+1)!}\sum_{r=0}\frac{(n)_r}{r!}\left[\frac{1}{\xi}\right]^r\mathcal{F}_{yz}^{(r,s)}(y,z)\ , \tag{A11}$$

in which the function $\mathcal{F}_{yz}^{(r,s)}(y,z)$ is defined by

$$\mathcal{F}_{yz}^{(r,s)}(y,z)=\frac{\partial^r}{\partial y^r}\frac{\partial^s}{\partial z^s}\mathcal{F}(y,z)\ . \tag{A12}$$

In a similar manner one can establish that for $n\geq 1$,

$$\varphi_n=\sum_{u=0}\left[\frac{(n)_u}{u!}\right]^2\left[\frac{1}{(n+1)!}\right]^2\left[\frac{1}{\xi}\right]^{2u}\mathcal{B}^{(2u)}(y)\ . \tag{A13}$$

It is readily seen that the function $\mathcal{B}_y^{(2u)}(y)$ represents the partial derivative of order $2u$ for $\mathcal{B}(y)$ with respect to the independent variable $y$.


[1] T. M. Reed and K. E. Gubbins, in *The Thermodynamic and Transport Properties of Fluids* (Butterworth, Washington, DC, 1991).

[2] H. Falkenhagen and W. Ebling, in *Ionic Interactions,* edited by S. Petrucci (Academic, New York, 1971), Chap. 1.

[3] M. P. Taylor and J. E. G. Lipson, J. Chem. Phys. **97**, 4301 (1992).

[4] P. Sloth and T. S. Sorensen, J. Phys. Chem. **94**, 2116 (1990).

[5] R. J. Wheaton, J. Chem. Soc. Faraday Trans. 2 **76**, 1093 (1980).

[6] R. J. Wheaton, J. Chem. Soc. Faraday Trans. 2 **76**, 1599 (1980).

[7] R. J. Wheaton, J. Chem. Soc. Faraday Trans. 2 **77**, 673 (1981).

[8] R. J. Wheaton, J. Chem. Soc. Faraday Trans. 2 **77**, 1343 (1981).

[9] G. Arfken, *Mathematical Methods of Physicists* (Academic, New York, 1985).

[10] D. N. Card and J. P. Valleau, J. Chem. Phys. **52**, 6232 (1970).

[11] J. P. Valleau, L. K. Cohen, and D. N. Card, J. Chem. Phys. **72**, 5942 (1980).

[12] G. Schmitz, Phys. Lett. **21**, 174 (1966).

[13] G. Schmitz, Ann. Phys. (Leipzig) **21**, 31 (1968).

[14] N. N. Bogoliubov, in *Studies in Statistical Mechanics,* edited by J. de Boer and G. E.Uhlenbecker (North-Holland, Amsterdam, 1962), Vol. 1.

[15] H. Falkenhagen, W. Ebeling, and H. G. Hertz, *Theorie der Electrolyte* (Hirzel, Leipzig, 1970).

[16] W. Ebeling and H. Krienke, Z. Phys. Chem. **248**, 274 (1971).

[17] W. H. Lee and R. J. Wheaton, J. Chem. Soc. Faraday Trans. 2 **74**, 743 (1978).

[18] J. P. Valleau and L. K. Cohen, J. Chem. Phys. **72**, 5935 (1980).